HTS MODELLING WORKGROUP

9th International Workshop on Numerical Modelling of High Temperature Superconductors - HTS 2024

10-13 June 2024, Bad Zurzach, Switzerland

Influence of ferromagnetic structure addition on the field trapping ability of MgB_2 bulk samples

Laura Gozzelino, Michela Fracasso, Roberto Gerbaldo

Politecnico di Torino

Politecnico di Torino,
Department of Applied Science and Technology
and INFN Sez. Torino, Torino, Italy

INFN Istituto Nazionale di Fisica Nucleare SEZIONE DI TORINO

Yiteng Xing, Pierre Bernstein, Jacques Noudem

UMR 6508, CRISMAT, ENSICAEN, CNRS, UNICAEN, France

Outline

- ❖ Motivation and background
- ❖ Trapped field in MgB_2 discs
  - ✓ Sample and measurement details
  - ✓ Experimental results
  - ✓ Numerical modelling
    - → critical current density calculation
  - ✓ Comparison between experimental and computation results
- ❖ Numerical analysis of the trapping field ability of new hybrid (SC/FM) layouts of permanent magnets
- ❖ Conclusions

Investigating and predicting the magnetization of bulk superconductors

➢ **is crucial to using them as:**

- quasi-permanent magnets
- magnetic shields

- magnetic bearings,
- energy storage flywheels,
- magnetic resonance imaging,
- magnetic separation
- rotating machines (motors/generators)

J.H. Durrell et al., *Supercond. Sci. Technol.* 31 (2018) 31
B. Douine et al., *Materials* 14 (2021) 1636

key materials for the energy transition

➢ **requires:**

manufacturing techniques able to provide suitably shaped objects

modelling procedures able to guide the devices optimization depending on the required working conditions

Field trapping ability of bulk superconductors

superconducting (SC) materials

SC cuprates (YBCO, ReBCO)

M. Tomita et al., *Nature* 421 (2003) 517
D.M. Ainslie et al, *SuST* 29 (2016) 124004
D.M. Ainslie et al, *SuST* 32 (2019) 034002
H. Fujishiro et al., *SuST* 32 (2019) 045005
Y.L. Cui et al., *SuST* 33 (2020) 025011
M. Houbart et al., *SuST* 33 (2020) 064003
T. Motoki et al., *SuST* 35 (2022) 094003
CAN SUPERCONDUCTORS - https://www.can-superconductors.com

MgB_2

G. Fuchs et al., SuST 26 (2013) 122002.
A. Yamamoto et al., *APL* 105 (2014) 032601.
V. Cientanni et al., *SuST* 34 (2021) 114003
M. Muralidhar et al, *J. Phys. D: Appl. Phys.* 57 (2023) 053001.
M. Fracasso et al., *Materials* 17 (2024) 1201

- low fabrication costs
- low weight density
- working temperature easily achievable using cryogen free cryocoolers
- long coherence length
- **growth techniques allowing the fabrication of suitably shaped samples**

e.g. - manufacturing near net-shape MgB_2 bulks

G. Giunchi et al., *Cryogenics* 46 (2006) 237
A. G. Bhagurkar et al., *SUST* 28 (2015) 015012
D. A. Moseley et al., *SUST* 35 (2022) 085003

- manufacturing fully machinable MgB_2 bulks

P. Badica at al., *Supercond. Sci. Technol.* 27 (2014) 095013
L. Gozzelino et al., *SUST* 33 (2020) 044018

- soldering MgB_2 bulks

Y. Thimont et al., *Coatings* 12 (2022), 1151

MgB_2 fabrication process

- Commercial powders of MgB_2 powder (purity >97%, 100 meshes)
- Spark plasma sintering (SPS) was applied on the powder to produce a high-density bulk disks with a diameter of 20 mm. SPS temperature was 1200° C for a dwell time of 10 min. The maximum pressure applied on the sample during sintering was 50 Mpa under a dynamic vacuum of 10^{-3} bar.

Y. Xing at al., *Supercond. Sci. Technol*. 36 (2023) 115005

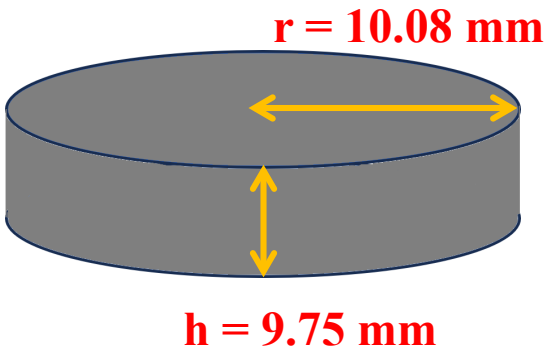

T_c = 38.5 K

Measurement set-up

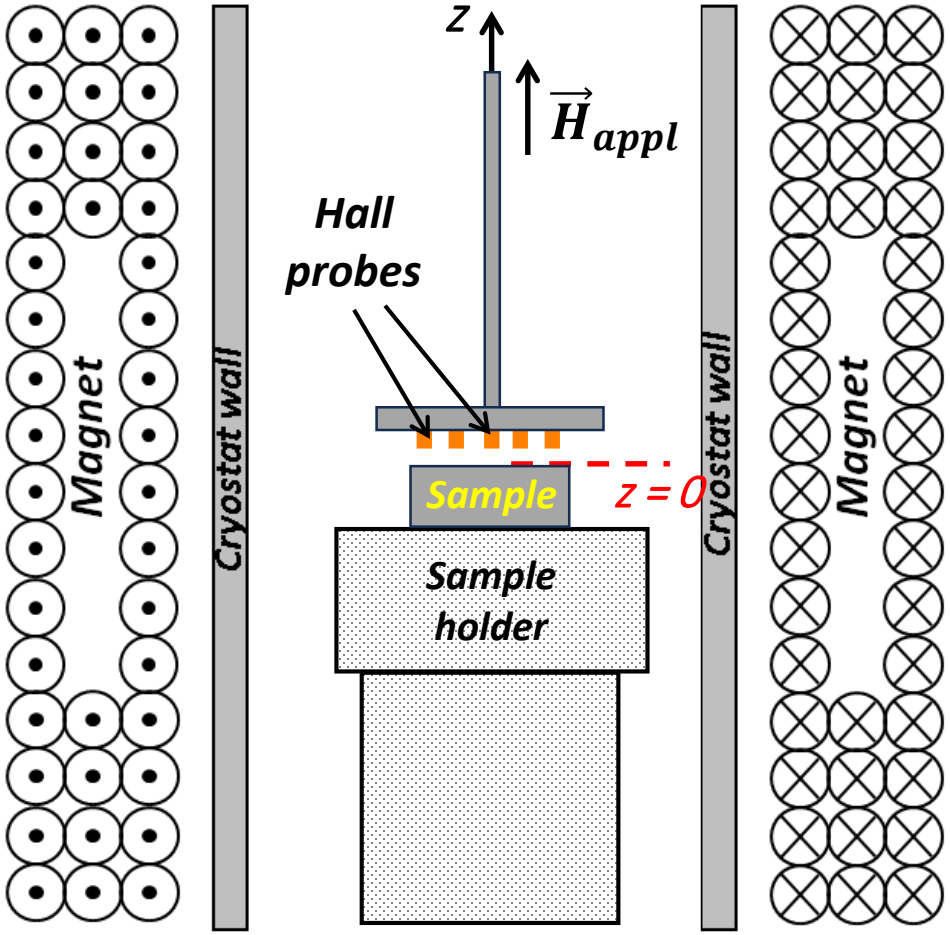

Field cooling in an external applied field

$\mu_0 H_{appl} = 4T$

Measurement details

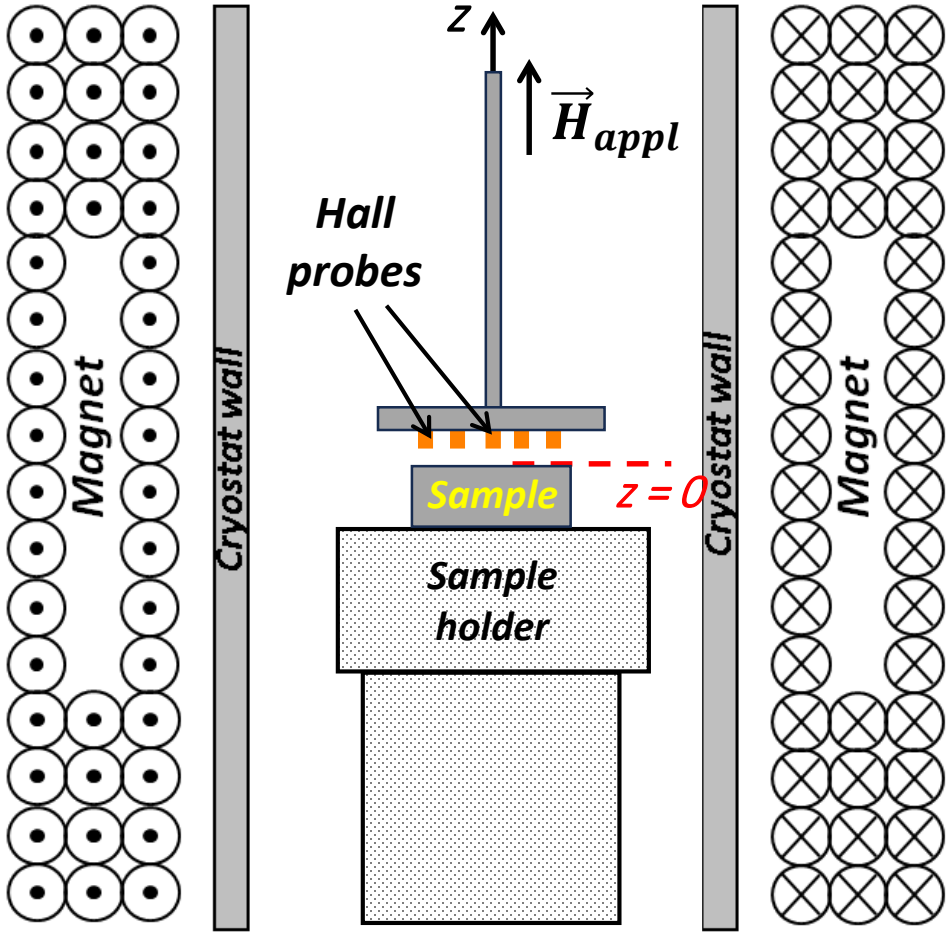

Field cooling in an external applied field

$\mu_0 H_{appl} = 4T$

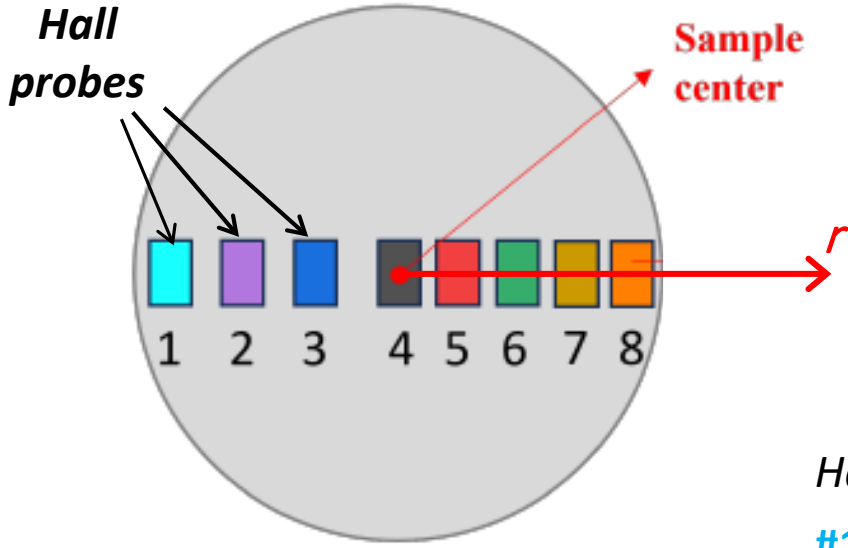

Hall probes distributed along the disc's diameter:

Magnetic flux density measured:

- *during the external field removal*
- *in remnant state as a function of the distance from the sample surface*

$B_{trapped,z} = B_z - \mu_0 H_{appl}$

Hall probes positions

#1: r = - 8.0 mm
#2: r = - 5.75 mm
#3: r = - 3.5 mm
#4: r = 0.0 mm (sample center)
#5: r = + 2.0 mm
#6: r = + 4.0 mm
#7: r = + 6.0 mm
#8: r = + 8.5 mm

Experimental results

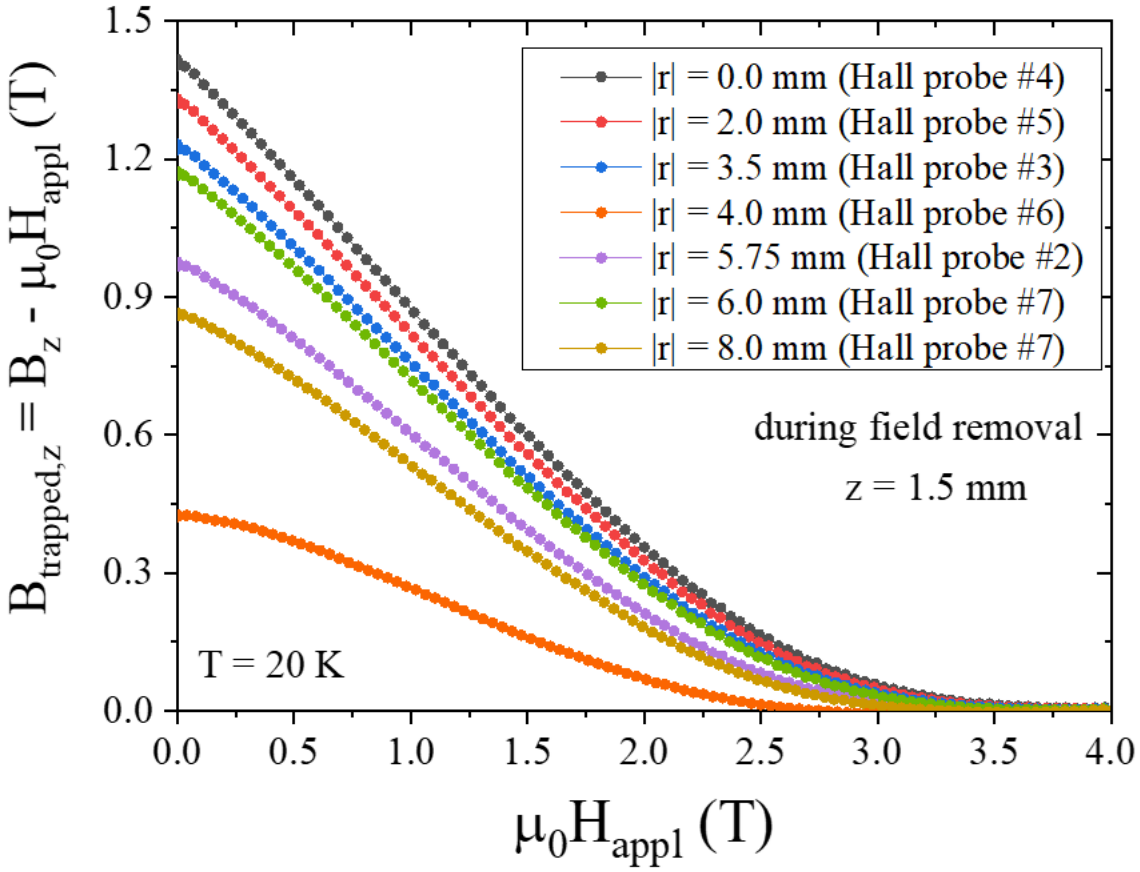

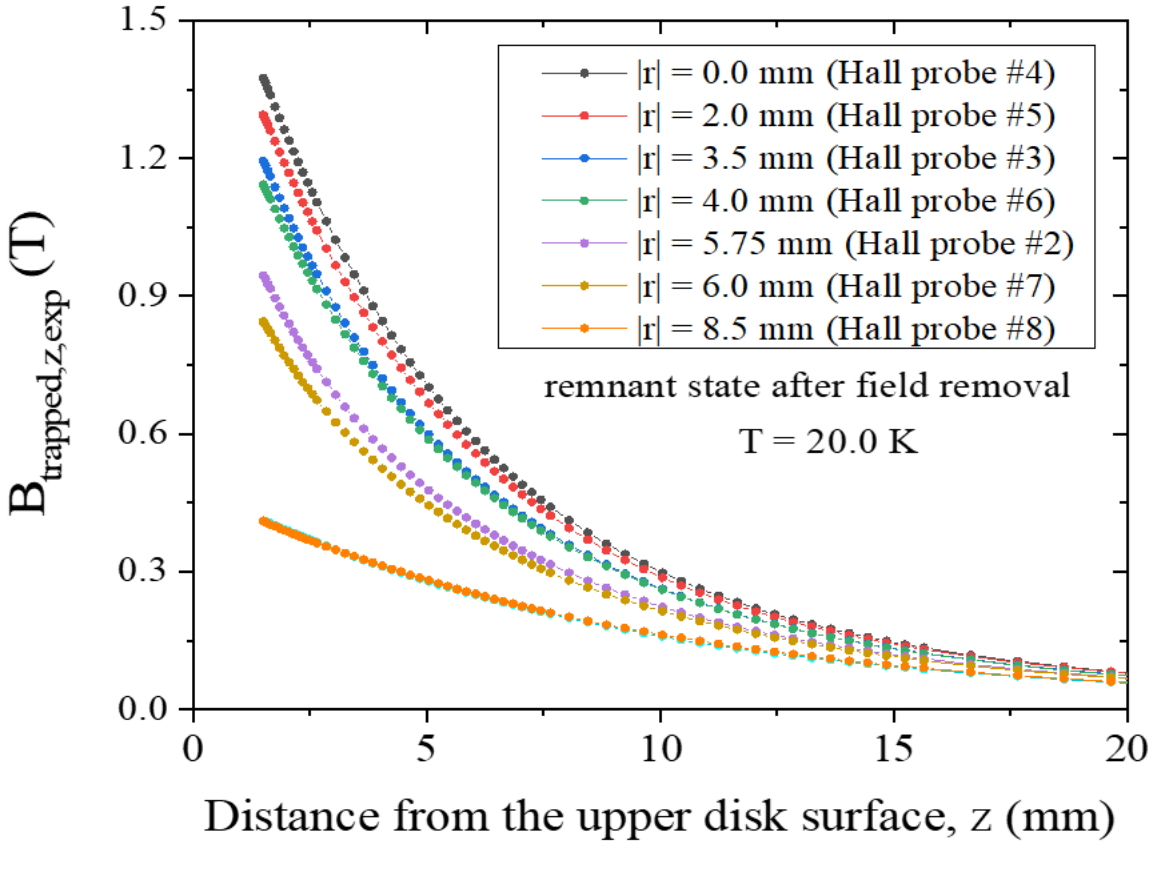

- Trapped field ~ 1.4 T (z = 1.5 mm, r = 0)
- Further improvement via ferromagnetic bulk addition ?

M. Fracasso et al., *Materials* 17 (2024) 1201

Effect of ferromagnetic structure addition

Addition of ferromagnetic structure is expected to improve the field trapping ability of a superconductor

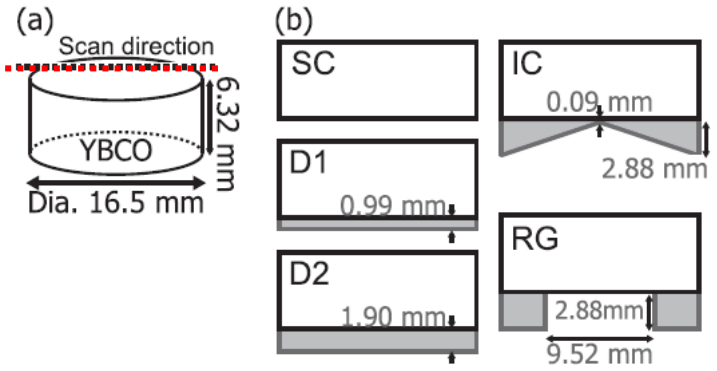

YBCO – 77 K

M P Philippe et al., *SuST* 28 (2015) 095008.

$B_{trapped,z}$ at z =0.85 mm above the external surface

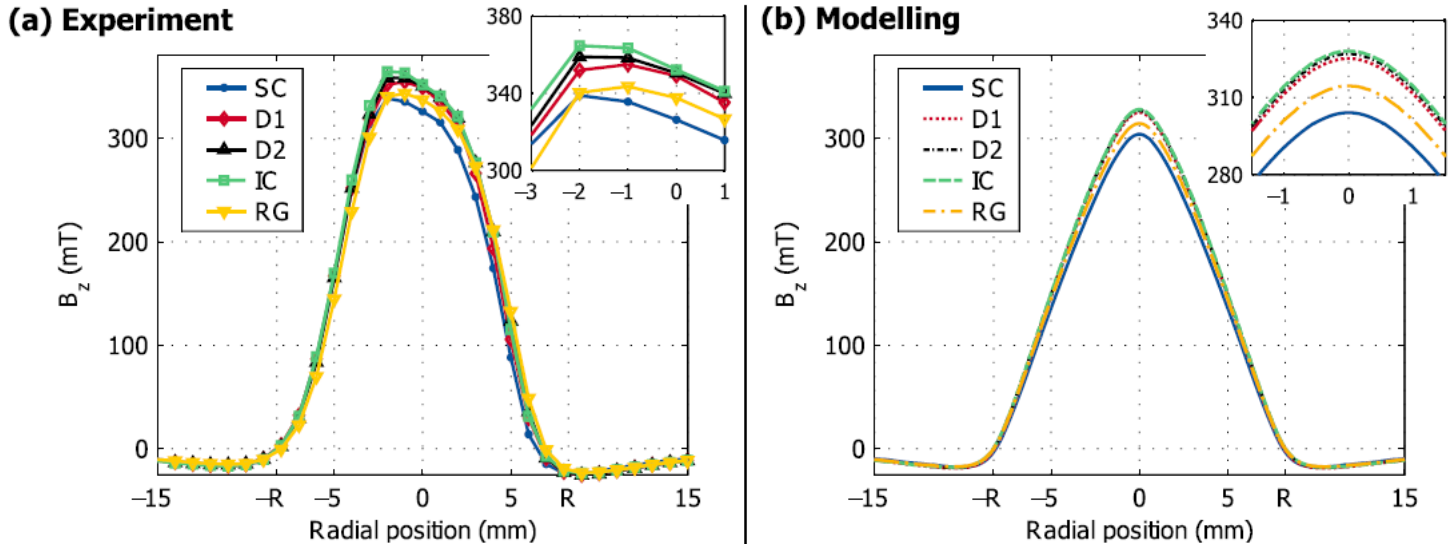

YBCO – 77 K

R. Li et al, IEEE TAS 33 (2023) 6801206

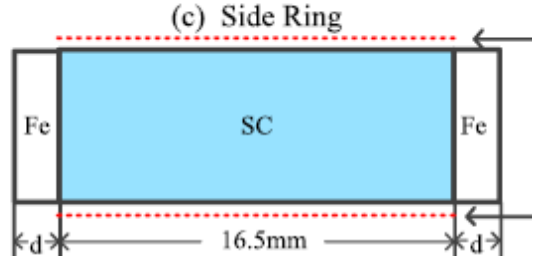

$B_{trapped,z}$ at z =1.0 mm above the external surface

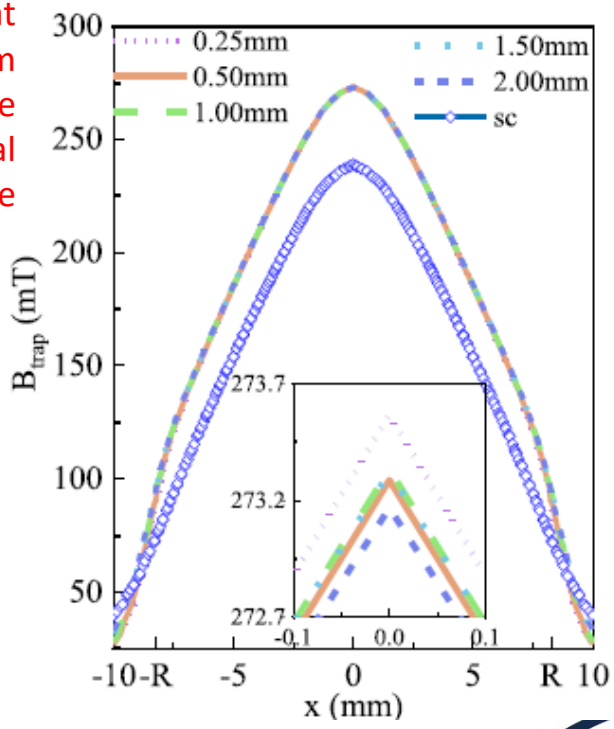

Modelling

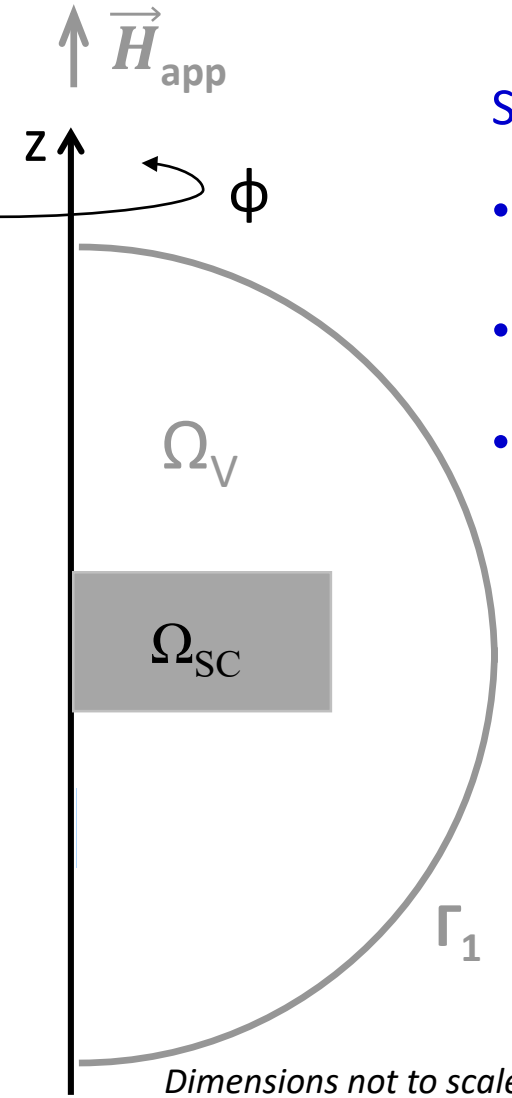

Dimensions not to scale

Superconductor ***magnetic modelling*** (2D axisymmetric approach):

- $\vec{A}$-formulation based procedure — A.M. Campbell, *SuST* 20 (2006) 292; F. Gömöry et al., *SuST* 22 (2009) 034017
- The local electric field $\vec{E}$ is defined by the time evolution of $\vec{A}$: $\boldsymbol{E_\phi = -\partial A_\phi / \partial t}$
- E-J relation smoothly approximating the critical state model

$$J_\phi = J_c(B) \tanh\left(\frac{|E_\phi|}{E_c}\right)$$

M. Solovyov and F. Gomory, *SuST* 32 (2019) 115001

Boundary condition (Γ_1): the field was assumed constant and equal to $\mu_0 \vec{H}_{app}$ (decreasing with a ramp rate of 0.35 T/s from an initial value of 4.0 T).

J_c calcolation

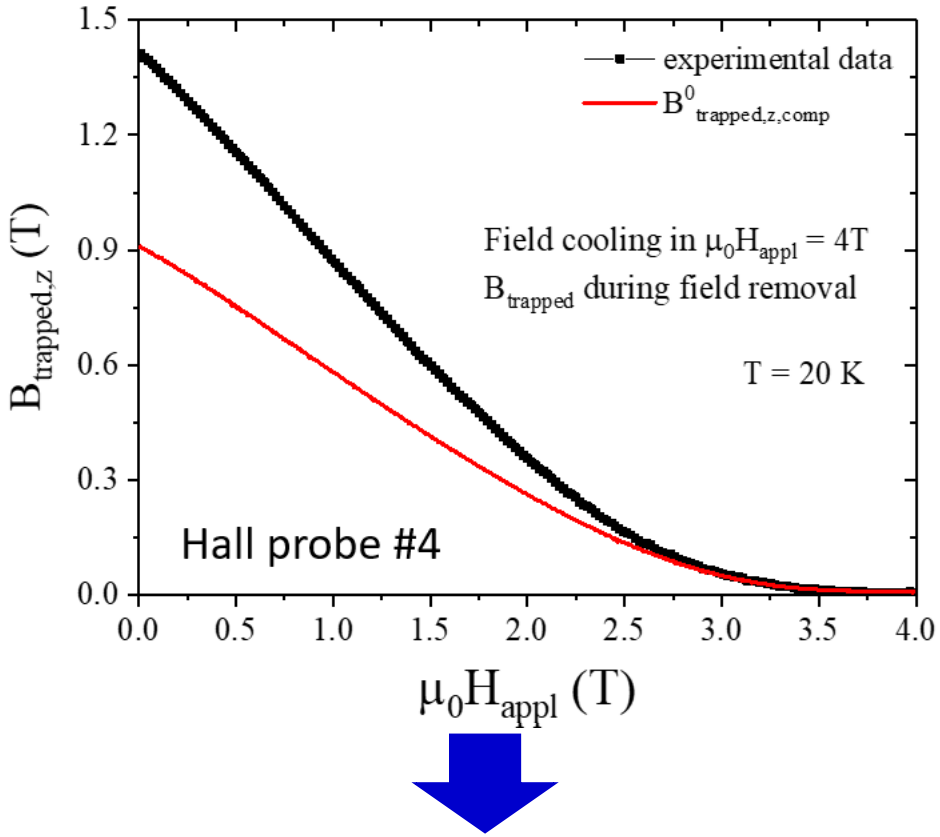

Polynomial fit ➔ $J_c(B)$ inserted in

$$J_\phi = J_c(B)\tanh\left(\frac{|E_\phi|}{E_c}\right)$$

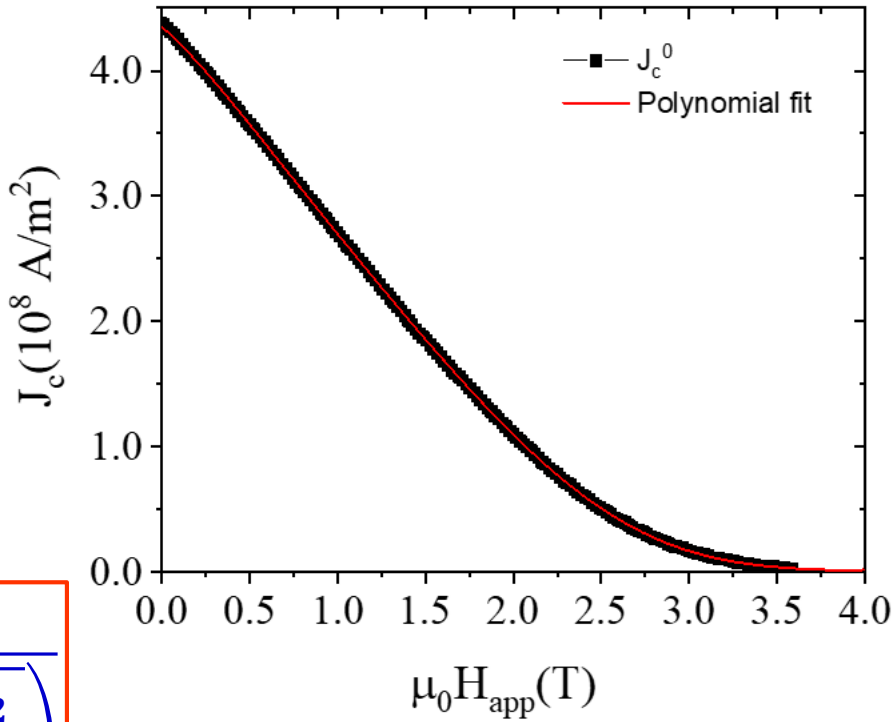

$$J_c^0 = \frac{2B_{trapped}}{\mu_0}\frac{1}{(z+h)\,ln\left(\frac{R}{z+h}+\sqrt{1+\frac{R^2}{(z+h)^2}}\right)-(z)\,ln\left(\frac{R}{z}+\sqrt{1+\frac{R^2}{(z)^2}}\right)}$$

R *and* ***h*** *are the radius and the height of the disc and* ***z*** *is the distance from the top of the sample*

I.G. Chen et al., *J. Appl. Phys.*, 72 (1992) 1013

J_c calcolation

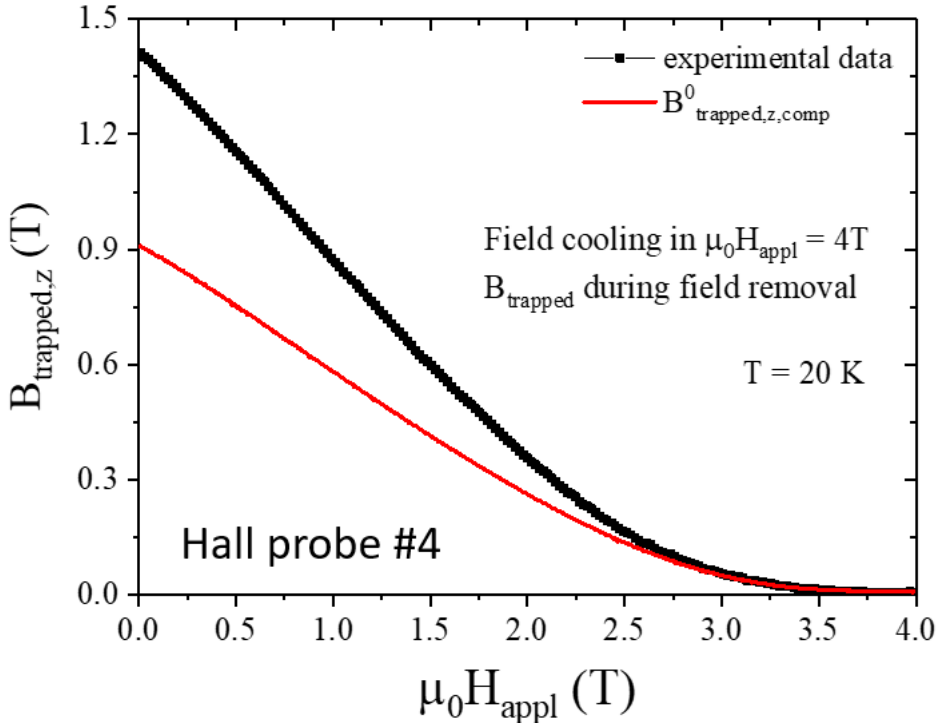

Computation based on the Bean model underestimates J_c (B) when the applied field is lower than the full penetration one.

D.X. Chen et al., J. Appl. Phys. 66 (1989) 2489

Iterative procedure for J_c calculation

M. Fracasso et al., *Materials* 17 (2024) 1201

J_c calculation

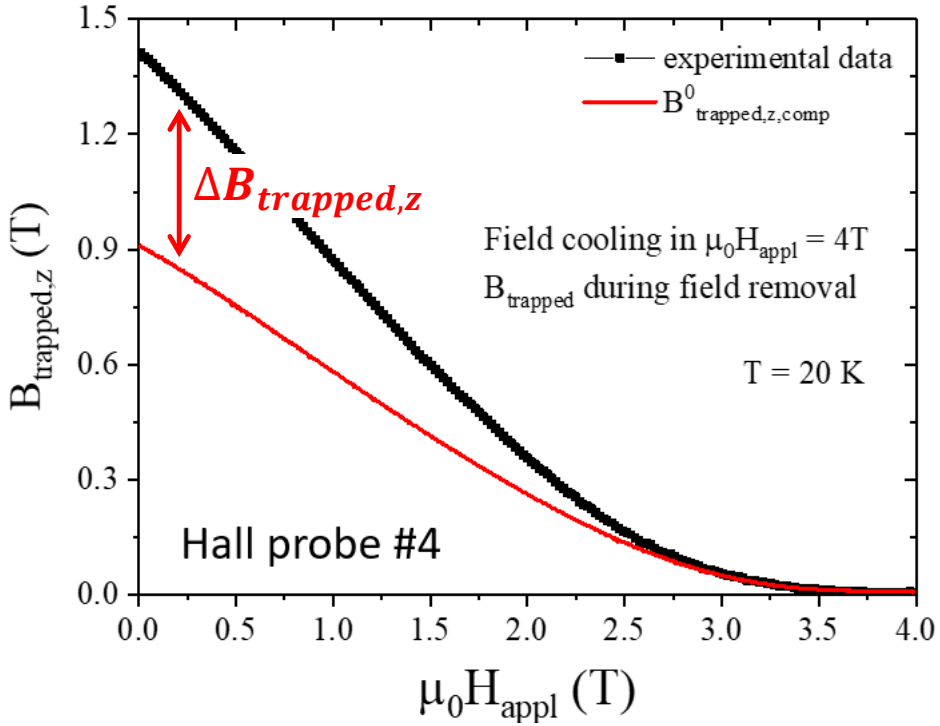

Difference between the computed and the experimental data

$$\Delta B^0_{trapped,z} = B_{trapped,z,exp} - B^0_{trapped,z,comp}$$

$$\Delta J^0_c = \frac{2\Delta B_{trapped,z}}{\mu_0} \frac{1}{(z+h)\, ln\left(\frac{R}{z+h} + \sqrt{1+\frac{R^2}{(z+h)^2}}\right) - (z)\, ln\left(\frac{R}{z} + \sqrt{1+\frac{R^2}{(z)^2}}\right)}$$

$$J^1_c = J^0_c + \Delta J^0_c$$

Polynomial fit of J^1_c vs. $\mu_0 H_{appl}$ ➔ inserted in $J_\phi = J^1_c(B)\, tanh\left(\frac{|E_\phi|}{E_c}\right)$

➔ $E_\phi = -\frac{\partial A_\phi}{\partial t}$ ➔ $B^1_{trapped,z,comp}$

M. Fracasso et al., *Materials* 17 (2024) 1201

J_c calculation

Difference between the computed and the experimental data

$$\Delta B^0_{trapped,z} = B_{trapped,z,exp} - B^0_{trapped,z,comp}$$

$$\Delta J^0_c = \frac{2\Delta B_{trapped,z}}{\mu_0} \frac{1}{(z+h)\, ln\left(\frac{R}{z+h} + \sqrt{1+\frac{R^2}{(z+h)^2}}\right) - (z)\, ln\left(\frac{R}{z} + \sqrt{1+\frac{R^2}{(z)^2}}\right)}$$

$$J^1_c = J^0_c + \Delta J^0_c$$

Polynomial fit of J^1_c vs. $\mu_0 H_{appl}$ ➔ inserted in $J_\phi = J^1_c(B)\, tanh\left(\frac{|E_\phi|}{E_c}\right)$

➔ $E_\phi = -\frac{\partial A_\phi}{\partial t}$ ➔ $B^1_{trapped,z,comp}$

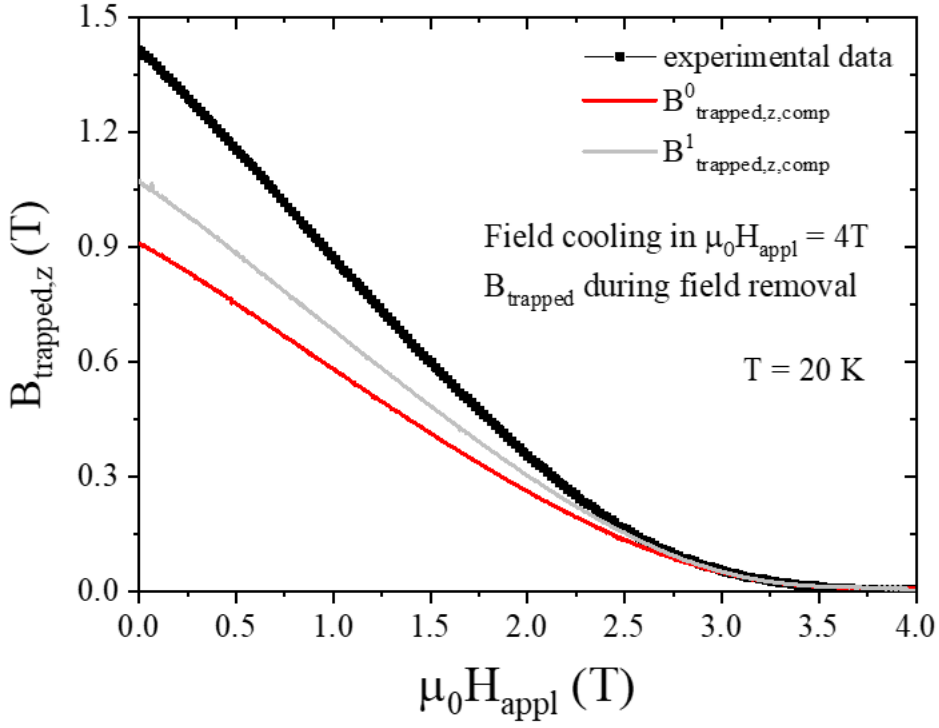

M. Fracasso et al., *Materials* 17 (2024) 1201

J_c calculation

Difference between the computed and the experimental data

$$\Delta B^i_{trapped,z} = B_{trapped,z,exp} - B^i_{trapped,z,comp}$$

$$\Delta J^i_c = \frac{2\Delta B^i_{trapped,z}}{\mu_0} \frac{1}{(z+h)\, ln\left(\frac{R}{z+h} + \sqrt{1+\frac{R^2}{(z+h)^2}}\right) - (z)\, ln\left(\frac{R}{z} + \sqrt{1+\frac{R^2}{(z)^2}}\right)}$$

$$J_c^{i+1} = J_c^i + \Delta J_c^i$$

Polynomial fit of J_c^{i+1} vs. $\mu_0 H_{appl}$ ➔ inserted in $J_\phi = J_c^{i+1}(B)\, tanh\left(\frac{|E_\phi|}{E_c}\right)$

➔ $E_\phi = -\frac{\partial A_\phi}{\partial t}$ ➔ $B^{i+1}_{trapped,z,comp}$

J_c calculation

Difference between the computed and the experimental data

$$\Delta B^i_{trapped,z} = B_{trapped,z,exp} - B^i_{trapped,z,comp}$$

$$\Delta J^i_c = \frac{2\Delta B^i_{trapped,z}}{\mu_0} \frac{1}{(z+h)\, ln\left(\frac{R}{z+h} + \sqrt{1+\frac{R^2}{(z+h)^2}}\right) - (z)\, ln\left(\frac{R}{z} + \sqrt{1}\right.}$$

$$J_c^{i+1} = J_c^i + \Delta J_c^i$$

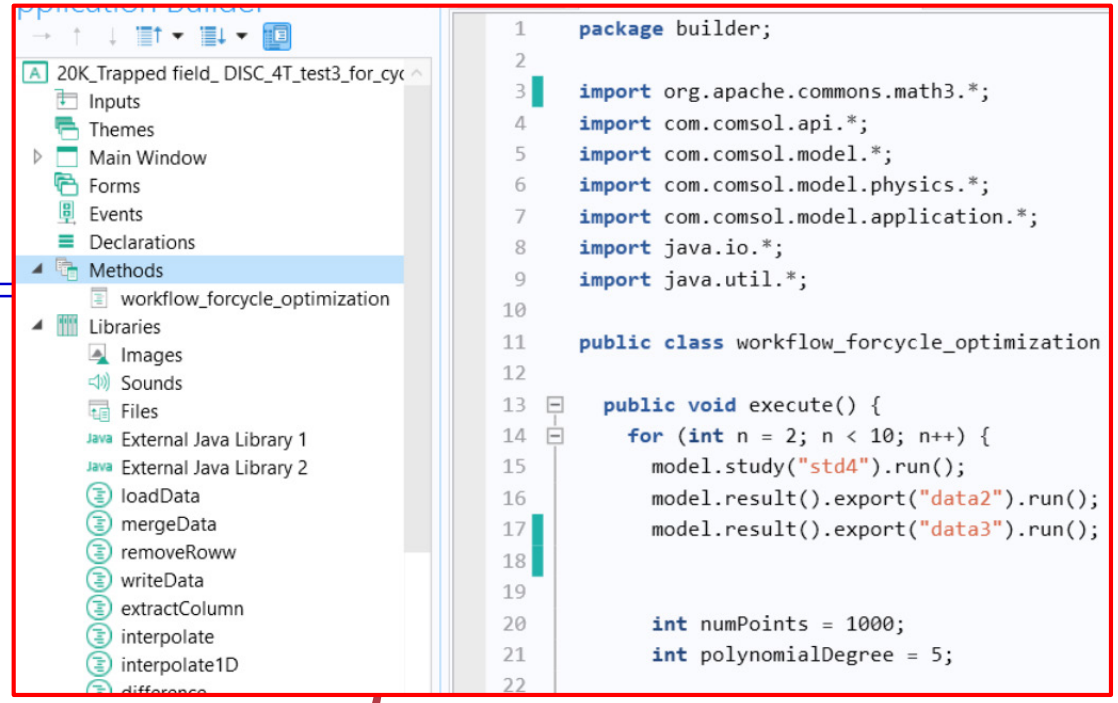

Polynomial fit of J_c^{i+1} vs. $\mu_0 H_{appl}$ ➔ inserted in $J_\phi = J_c^{i+1}(B)\, tanh\left(\frac{|E_\phi|}{E_c}\right)$

➔ $E_\phi = -\frac{\partial A_\phi}{\partial t}$ ➔ $B^{i+1}_{trapped,z,comp}$

J_c calculation

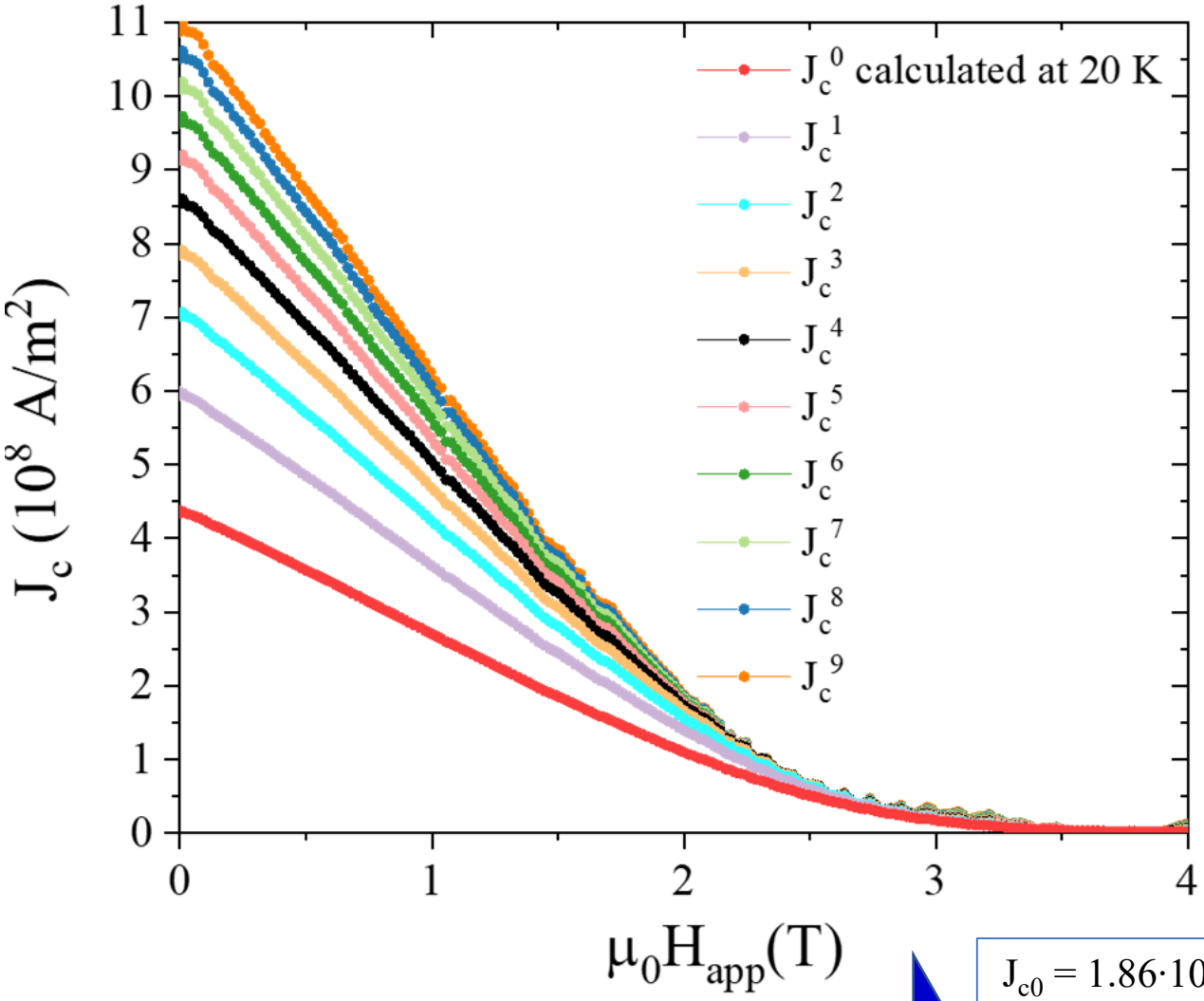

J_c^{i+1}

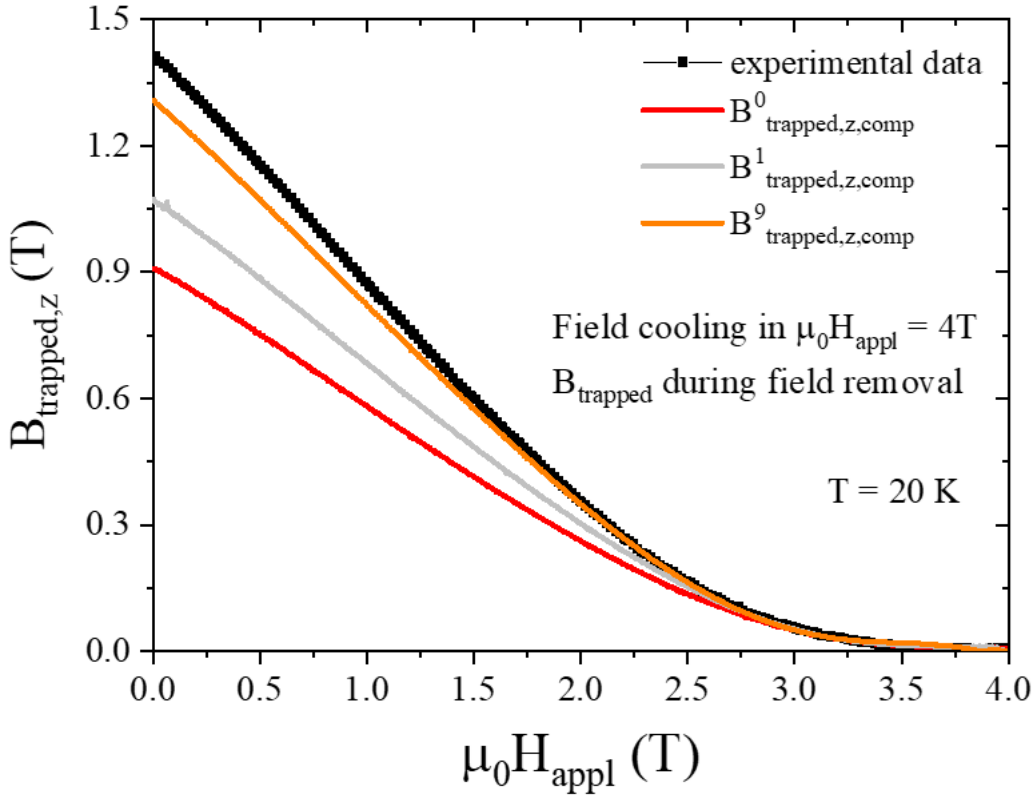

The last iteration was fitted by $J_c^{exp}(B) = J_{c,0} exp\left[-\left(\frac{B}{B_0}\right)^{\gamma}\right]$

M. Fracasso et al., *Materials* 17 (2024) 1201

$J_{c0} = 1.86 \cdot 10^9$ A/m^2
$B_0 = 1.21$ T
$\gamma = 1.66$

$$J_\phi = J_c^{exp}(B) tanh\left(\frac{|E_\phi|}{E_c}\right)$$

L. Gozzelino et al., *SuST* 35 (2022) 044002

Comparison between experimental and computational results

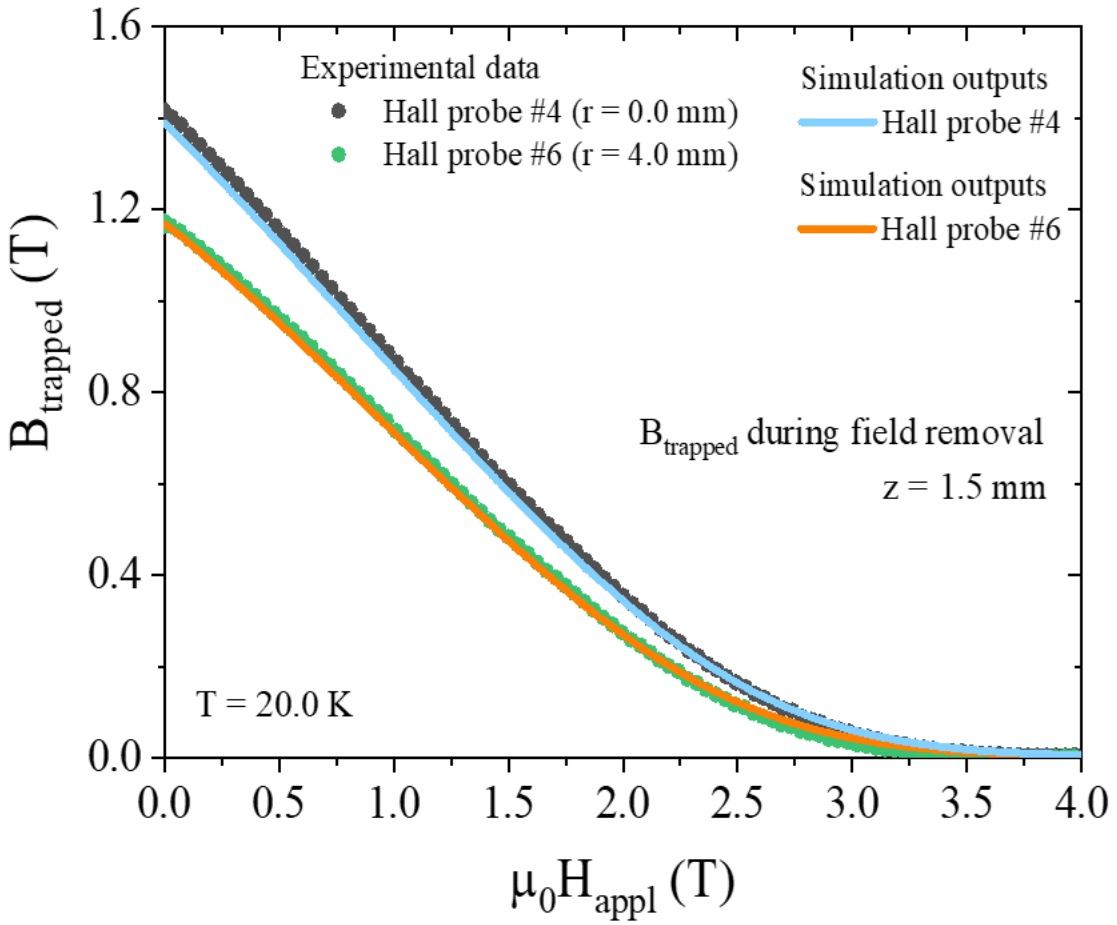

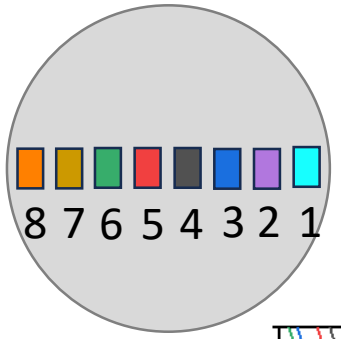

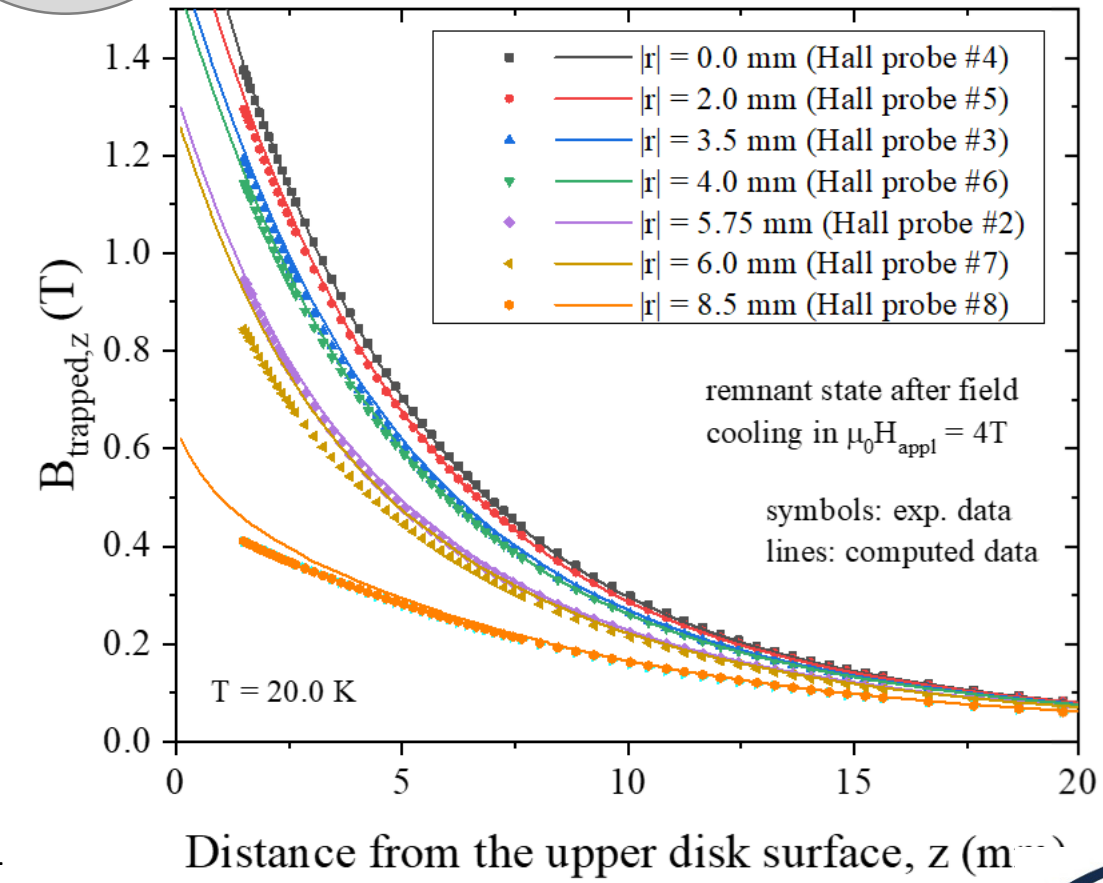

REMARKABLE AGREEMENT!

M. Fracasso et al., *Materials* 17 (2024) 1201

Modelling

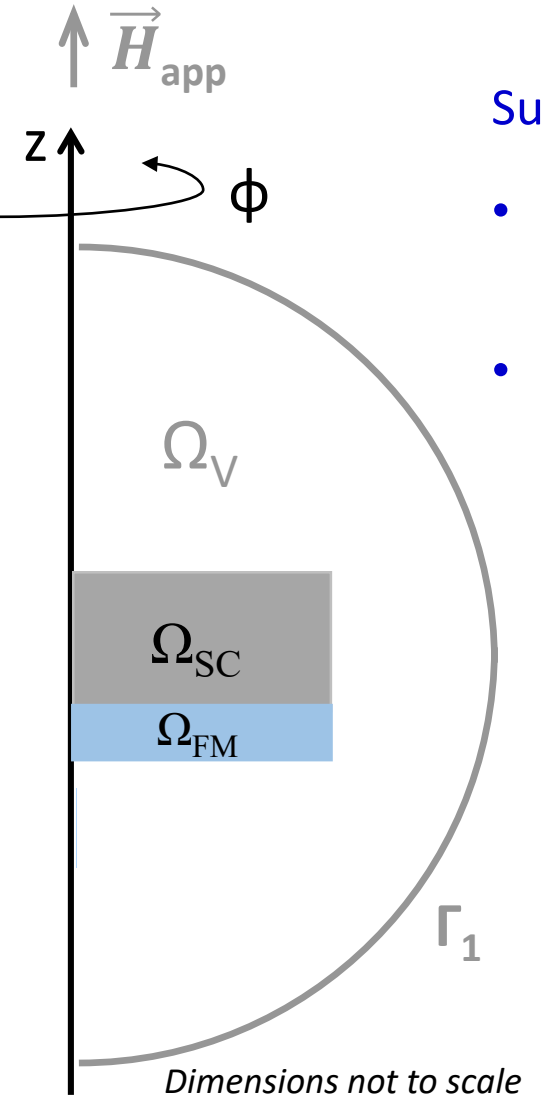

Dimensions not to scale

Superconductor ***magnetic modelling*** (2D axisymmetric approach):

- $\vec{A}$-formulation based procedure A.M. Campbell, *SuST* 20 (2006) 292
  F. Gömöry et al., *SuST* 22 (2009) 034017
- E-J relation smoothly approximating the critical state model

$$J_\phi = J_c(B)\tanh\left(\frac{|E_\phi|}{E_c}\right)$$

$$J_c(B) = J_{c,0}\exp\left[-\left(\frac{B}{B_0}\right)^\gamma\right]$$

$J_{c0} = 1.86\cdot10^9$ A/m^2
$B_0 = 1.21$ T
$\gamma = 1.66$

  - To model the **ferromagnetic material (soft iron) :**
    - $\vec{A}$-formulation
    - *B-H* curve measured experimentally
      - negligible hysteresis losses

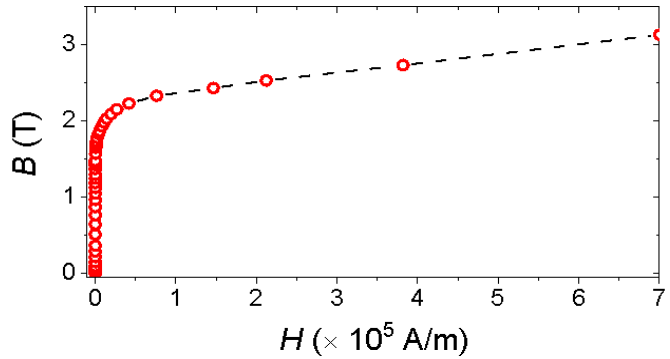

Boundary condition (Γ_1): the field was assumed constant and equal to $\mu_0\vec{H}_{app}$ (decreasing with a ramp rate of 0.35 T/s from an initial value of 4.0 T).

Effect of ferromagnetic structure addition

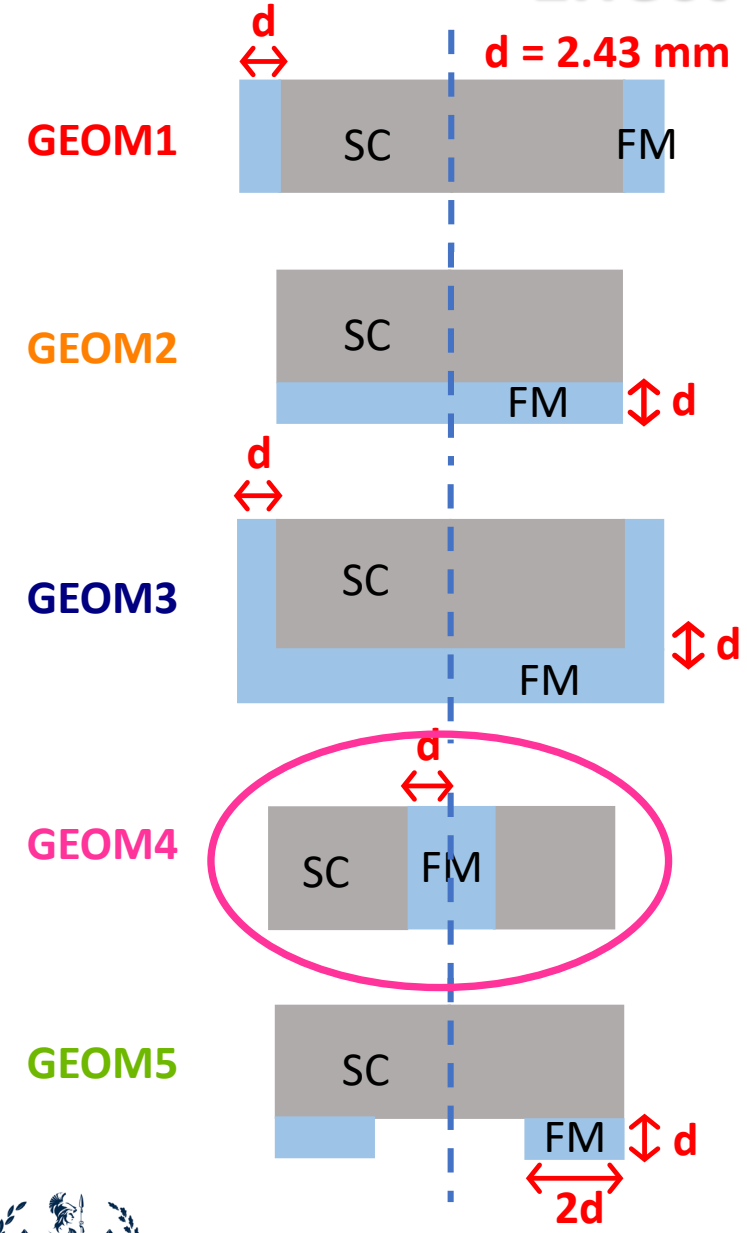

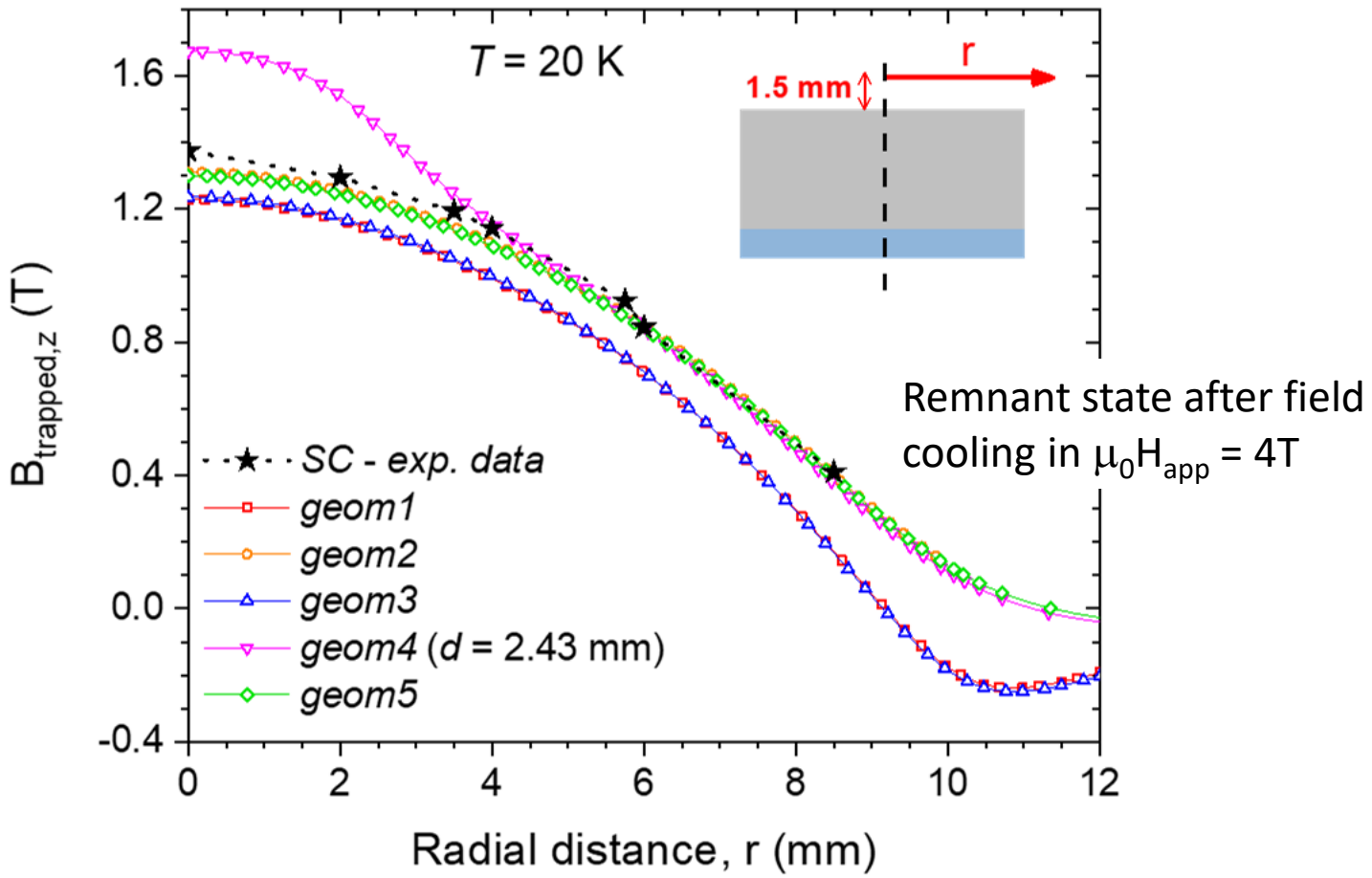

Remnant state after field cooling in $\mu_0 H_{app}$ = 4T

GEOM4: maximum trapped flux density $B_{trapped,z}$ = 1.67 T at the position r = 0 mm, z = 1.5 mm

+ 19%

Effect of ferromagnetic structure addition

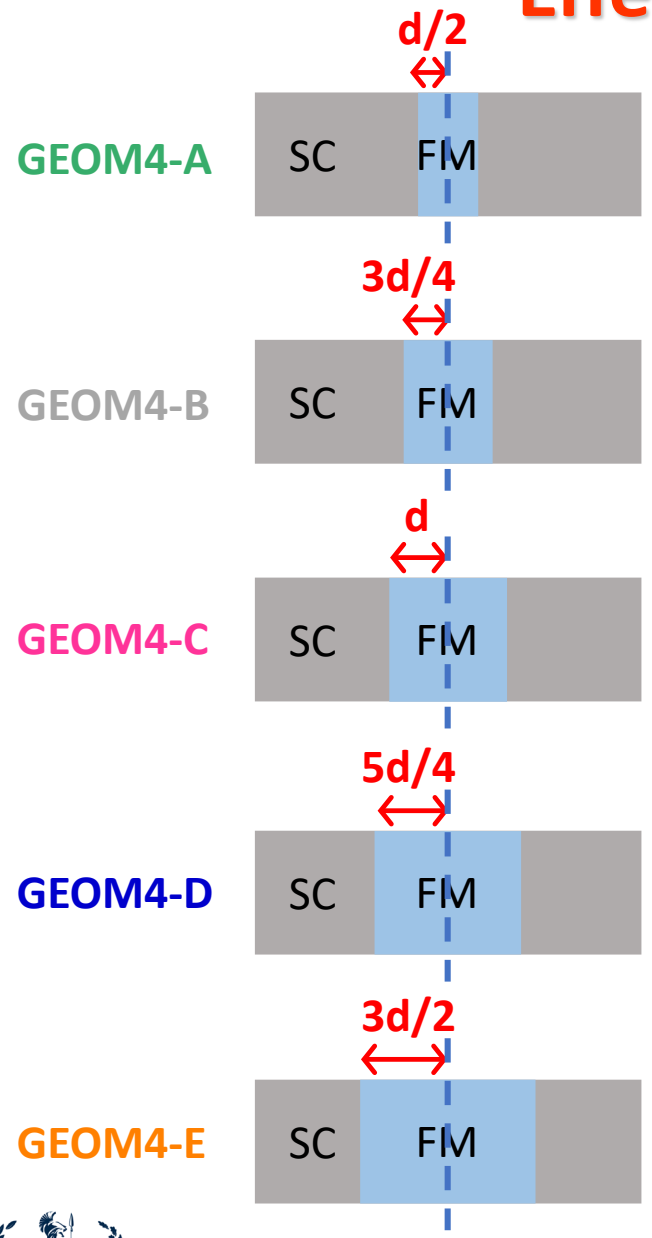

d = 2.43 mm

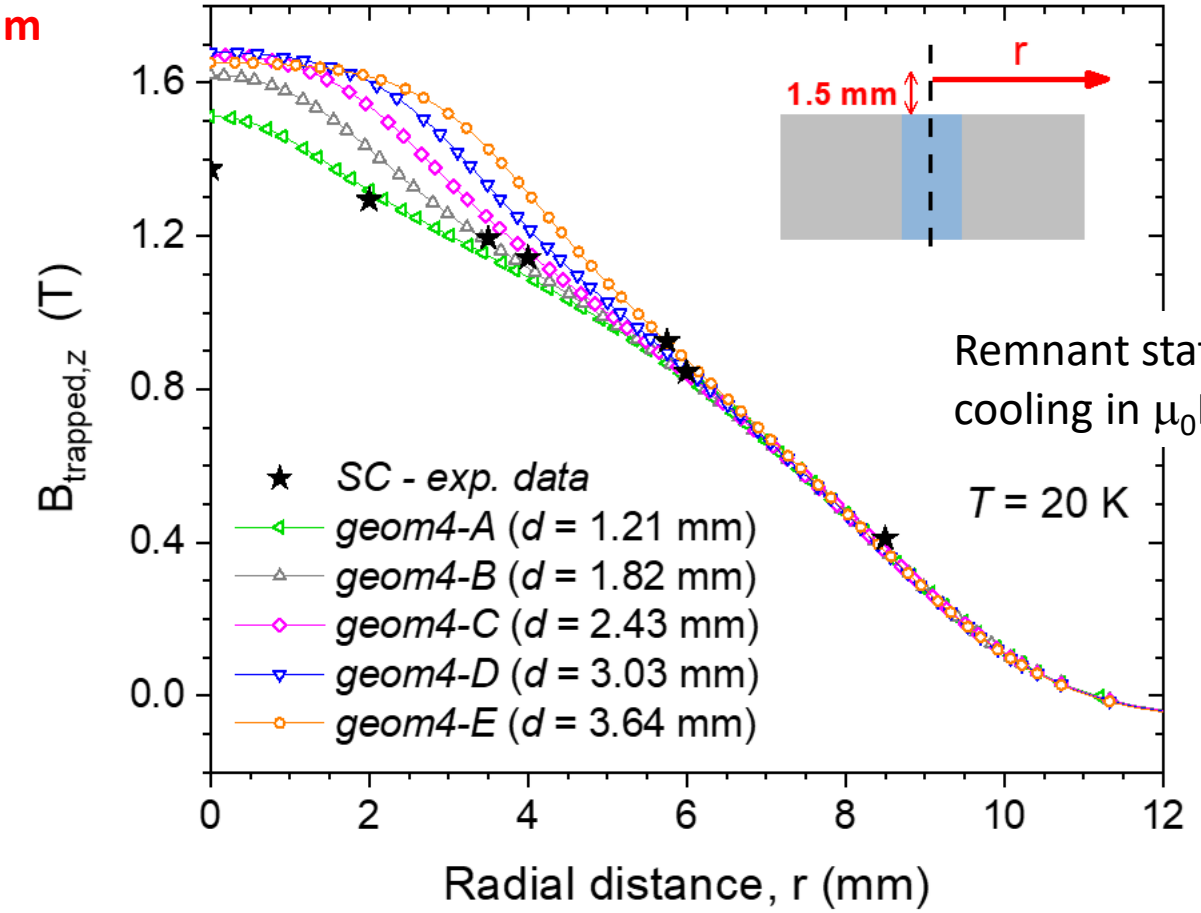

Remnant state after field cooling in $\mu_0 H_{app}$ = 4T

T = 20 K

The maximum trapped flux density is reached when the FM disc has a radius ranging between of d = 2.43 mm ($B_{trapped,z}$ = 1.67 T) and $4d/5$ = 3.03 mm ($B_{trapped,z}$ = 1.68 T)

GEOM4-C

GEOM4-B

Conclusions

❖ **Field trapping ability of MgB_2 discs** was experimentally investigated

➔ $B_{trapped,z}$ **~ 1.4 T**, at T = 20 K, along the disc's axis, 1.5 mm above its top surface

❖ **Experimental trapped field data are well reproduced by computation**

➔ **Critical current density evaluation from the trapped flux density curves through a suitably developed iterative process**

❖ **Field trapping ability of MgB_2 discs can be furtherly improved by ferromagnetic structure addition**

➔ Field trapping ability of hybrid magnet was investigated by numerical modelling

➔ **Enhancements up to ~ 20%** are predicted at 20 K, along the disc's axis, 1.5 mm above the surface

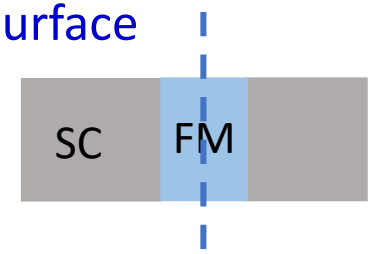

❖ **Further numerical investigations on hybrid permanent magnets with more complex geometries and subjected to different applied field orientations are on-going.**

Acknowledgements:

- G. Ghigo, F. Laviano, D. Torsello - *Politecnico di Torino*
- F. Gömöry and M. Solovyov - *Slovak Academy of Science*

Hi-SCALE Work partially supported by COST Action CA19108 (Hi-SCALE)

cost EUROPEAN COOPERATION IN SCIENCE & TECHNOLOGY

THANK YOU FOR YOUR KIND ATTENTION !